

Kinetics of thermally-induced conformational transitions in soybean protein films

Kun Tian^a, David Porter^b, Jinrong Yao^a, Zhengzhong Shao^a, Xin Chen^{a,*}

^aThe Key Laboratory of Molecular Engineering of Polymers of MOE, Department of Macromolecular Science, Laboratory of Advanced Materials, Fudan University, Shanghai 200433, People's Republic of China

^bDepartment of Zoology, University of Oxford, South Parks Road, Oxford, OX1 3PS, United Kingdom

ARTICLE INFO

Article history:

Received 16 October 2009

Received in revised form

22 February 2010

Accepted 22 March 2010

Available online 27 March 2010

Keywords:

Natural polymer

FTIR spectroscopy

Polymer–water interaction

ABSTRACT

The thermally-induced conformational transitions of soybean protein films were studied as the films were heated under isothermal conditions in the range 40–100 °C. By comparing the kinetics of protein–water interactions as a function of temperature using time-resolved Fourier transform infrared (FTIR) spectroscopy, thermogravimetric analysis (TGA), and dynamic mechanical thermal analysis (DMTA) measurements on soybean protein films, we have shown that simply evaporating water from the film (TGA) is insufficient to explain the rate of conformational changes (FTIR and DMTA). We suggest that an elastic instability condition of denaturation or glass transition events in water–amide interactions is the governing mechanism for conformational changes that allows the evolution of disordered structures into more ordered secondary structures, thereby controlling the changes in physical properties such as stiffness and water sensitivity.

© 2010 Elsevier Ltd. All rights reserved.

1. Introduction

Soybeans have a long history in the food industry owing to its high nutritional value and processability. However, soybean also contains a large fraction of proteins (up to 40%) [1] that has attracted research interest for the development of environment-friendly protein materials with potentially excellent physical properties like other natural polymers, such as cellulose [2] and chitosan [3,4]. Soybean protein isolate (SPI), more than 90% protein content, contains two major components: glycinin (11S, approximately 52% of the total protein content) and β -conglycinin (7S, approximately 35% of the total protein content) [5]. These two components are responsible for the nutritional, physicochemical and physiological properties of soybean proteins. A fundamental understanding of the conformation transitions of soybean protein and its sensitivity to processing and storage conditions will be very valuable for the preparation and application of natural protein materials in the future, as well as the more direct application to soy-based foodstuffs and environmentally friendly structural polymers.

More generally, properties such as water pick-up and mechanical properties of protein materials are often seen to change significantly over a period of minutes or hours after preparation, even under moderate laboratory conditions around ambient

temperature. This is qualitatively associated with a slow crystallization process. It is important as we try to develop reliable quantitative structure–property relations in proteins, such as regenerated silks for biomedical applications, if the materials are continuously changing. However, soybean protein films reported in earlier literature were blended with other polymers or plasticizers, such as PVA [6,7], wheat gluten [8], glycerol, diethylene glycol and ethylene glycol [9–11], etc., which were used for improving the limiting factors of the soybean protein films, such as poor mechanical properties, high water vapor permeability, and poor oxygen barrier properties. Furthermore, there is little reported on secondary structure changes in pure amorphous soybean protein films. We therefore attempted to monitor and quantify the conformational changes that take place in films of reconstituted soybean protein films as a function of temperature and time under these moderate conditions.

Fourier transform infrared (FTIR) spectroscopy is a powerful method to examine the secondary structure of proteins. The technique of time-resolved FTIR has been used for studying the kinetics of conformational transition process in silk protein solutions and films induced by potassium ions or ethanol [12–14] and more generally in polypeptide systems such as poly(aspartic acid) [15]. In a series of papers based on silk proteins, Hu et al. have shown how thermal properties, semicrystalline structure and FTIR spectra can be related quantitatively through the physics of the thermal energy associated with molecular vibrations [16–18]. The logic is that heat capacity in proteins is controlled by a combination of

* Corresponding author. Tel.: +86 21 65642866; fax: +86 21 51630300.
E-mail address: chenx@fudan.edu.cn (X. Chen).

atomic group and cooperative skeletal mode vibrations, as demonstrated by Wunderlich for polymers over many years [19]. These vibrations can be measured using FTIR spectroscopy and linked to the specific secondary structures (and hence the degree of crystallinity) found in proteins. In a similar approach, Porter has shown that the thermal energy components due to molecular vibrations can be used in a mean field potential function approach to predict the viscoelastic properties of polymers [20,21], including silk and other proteins [22,23]. Thus, all the main thermophysical properties of polymers and proteins in particular, can be linked quantitatively to structure at the molecular level.

The contribution of water to structure and properties in Hu's work is more elusive [17,18], although clear thermal events can be observed as discontinuous processes at temperatures around 70–100 °C, which can be associated with evaporation of water around transition processes at about 80 °C due to water kinetics in the protein. Such processes have been modelled as combinations of denaturing and local glass transition events in proteins, where hydrogen bonded water interactions with main chain amide groups in a protein become mobile at energy of an elastic instability condition, where the bond stiffness tends to zero [24]. At this point, the amide groups also become mobile and reconfigure to form stronger amide–amide hydrogen bonds associated with structures such as β -sheets.

The observations and relations shown by Hu et al. are based upon essentially 'static' or pseudo-equilibrium processes and properties. In order to further investigate the role of water in protein reconfiguration, we have looked at the temperature kinetics in proteins by three different techniques: FTIR, thermogravimetric analysis (TGA) and dynamic mechanical thermal analysis (DMTA). By comparing the kinetics at low temperatures (0–100 °C) associated with water effects, we hoped to better understand the role that water can play in the evolution kinetics of protein structure and properties; in particular the increase in crystalline β -sheet type structures.

2. Experimental section

2.1. Materials

Soybean protein isolate powder (Shanghai Shenyuan Food Co., Ltd.) was dissolved in 6 mol/L guanidine hydrochloride aqueous solution and then stirred at room temperature for 3 h while adding 0.01 mol/L 2-mercaptoethanol. After dialysis against NaOH aqueous solution (pH = 11.5) for two days and deionized water for another day at room temperature, the solution was centrifuged at a speed of 9000 rpm for 10 min to obtain a clear supernatant. The concentration of soybean protein solution was about 1.6% (w/w) analyzed by gravity method. To prepare films, the solution was first diluted to 0.8% (w/w). Then, 0.8 mL of this soybean protein solution was transferred to a 3 × 3 cm² polystyrene weighting boat and allowed to dry overnight at about 25 °C and 50% relative humidity. All of the films were dried under vacuum for two days. The thickness of the soybean protein films was about 6 μ m. This solution process has been described in detail elsewhere [25], and results in a very stable protein solution with almost no degradation of the protein chains relative to more conventional alkaline processes, for example, and is important for ongoing work on improved structural mechanical properties of soybean proteins.

2.2. Time-resolved FTIR analysis

The FTIR spectra were recorded using a Nicolet Nexus 470 FTIR spectrometer. To eliminate spectral contributions due to atmospheric water vapor, the instrument was continuously purged with

pure nitrogen gas (40 mL/min). All spectra were recorded in a variable-temperature cell with an accuracy of ± 0.1 °C. For each measurement, 64 interferograms were co-added and Fourier-transformed employing a Genzel-Happ apodization function to yield spectra with a nominal resolution of 4 cm⁻¹.

The thin soybean protein film was placed between a pair of NaCl windows in a variable temperature cell. For the time-resolved measurements, the film was heated quickly to 40, 50, 60, 70, 75, 80 and 100 °C respectively, and then the gathering of spectra was immediately initiated when the specified temperature was reached. Because the heating from room temperature to the elevated temperature needed about 2 min on average and the specified experimental parameters (64 scans per spectrum and the resolution of 4 cm⁻¹), the time of the start of spectra recording was set at 2 min, and the interval between two successive spectra was 0.67 min. The total data collection time was 60 min for each measurement.

Absorbance spectra at each temperature/time point were generated by dividing the single beam spectrum collected at a specific time by a background spectrum and converting to absorbance using OMNIC 5.1 (Microcal). The difference spectra were calculated by the subtraction of an absorbance spectrum collected at time *t* after heating the sample from the first absorbance spectrum. The data shown in the figures are from a single experiment, but closely similar results were obtained in replicates. Kinetics of the thermally-induced conformation transition was studied by fitting curves using Origin 7.5 (OriginLab Corporation). No smoothing was used for the equilibrium or kinetic difference spectra. All data reported in the text were the means and standard deviations for at least three separate runs.

2.3. TGA analysis

TGA measurements were taken in a Perkin Elmer Pyris 1 thermogravimetric analyser under nitrogen (40 mL/min). Before heating, the soybean protein sample was held for 3.0 min at 20 °C to remove the surface water under a nitrogen atmosphere. Isothermal experiments under low temperatures ranged from 20 to 100 °C were performed by heating at a fast rate to the specified temperature and then maintained at the certain temperature for 1 h until the water loss reached to the balance. Non-isothermal experiments were performed in the temperature range 20–700 °C, but only measurements up to 160 °C were used in this work. These experiments were performed at heating rates of 2, 5, 10 and 20 °C/min. All data reported in the text were the means and standard deviations for at least three separate runs.

2.4. DMTA analysis

DMTA measurements were run on a TA Q800 machine. The scans were run on the soybean film at a number of different heating rates (1, 2 and 5 °C/min) in the powder tray clamp in dual cantilever mode at 1 Hz. The samples in the powder tray (57 × 12 mm) were formed from multiple layers of the soybean films to a total thickness of about 35 μ m. Dried samples were stored under vacuum for 4 days at 20 °C with desiccant and more hydrated samples were left in different humidity conditions, although water content was not measured for these samples.

3. Results

3.1. Time-resolved FTIR analysis of soybean protein films

FTIR absorption spectra in the 1800–1400 cm⁻¹ region, which contains the most important band regions of amide I and amide II,

of the soybean protein films are shown in Fig. 1a during the conformation transition at various times at an example temperature of 100 °C. From our previous work on silk fibroin [12–14], we found that the conformation transitions of soybean protein films were similar to the conformational changes of silk fibroin induced by various exogenous factors, such as pH, metallic ions and organic solvents, etc. Thus, the development of the absorption bands in the amide I region could be assigned according to the literature on secondary structures of silk fibroin.

The amide I region between 1700 and 1600 cm^{-1} is commonly used for the evaluation of protein secondary structures, which originates mainly from the C=O stretching with some contribution from the N–H vibration. The region from 1640 to 1660 cm^{-1} includes contributions from random coils and α -helix structures in the silk fibroin [12–14,18]. The band from 1690 to 1700 cm^{-1} is classically assigned to weak β -sheet vibrations [16], but it seems better to be assigned to β -turns possibly together with a component derived directly from β -sheet according to our recent works [14,26].

The amide II region between 1600 and 1500 cm^{-1} is similarly dominated by chain oscillations, but the correlation between protein secondary structure and frequency is less straightforward than for the amide I vibration. The amide II bands are assigned to the coupling of the N–H in-plane bending and the C–N stretching vibration of the backbone, and also contain smaller contributions from the C=O in-plane bending and the C–C and N–C stretching vibrations [27–29]. A band around 1550 cm^{-1} is observed as an overlapped band of the amide II mode and is assigned to random

coil structures [30]. However, the origin of the amide II band at 1500 cm^{-1} was unknown. Around 1500 cm^{-1} , the band at 1515 cm^{-1} was attributed to different vibrational modes of Tyr side chains [28,29]. Hu et al. [18] suggested that the small shift and increase at the band of 1515 cm^{-1} reflects a reduction of conformational freedom as water is removed during heating the silk fibroin film. Generally, soybean protein contains about 4 mol% Tyr amino acid composition [31], similar to silk fibroin (4.8%) [32], so we should also observe a notable conformation transition in the amide II region during heating the soybean protein films under isothermal conditions. According to the results of our own experiments, we surmise that the amide II band at 1500 cm^{-1} should be assigned to β -turn or weak β -sheet structures although the evidence is still weak.

The changes in the absorption spectra can be visualized and examined more readily using difference spectra (Fig. 1b). In these difference spectra, the positive bands are attributable to developing structures, whereas negative intensities are due to vanishing structures. As the time increased, the amide I band absorption around 1650 cm^{-1} decreased considerably more rapidly than the coupled band around 1700 cm^{-1} increased. At the same time, the amide II band around 1550 cm^{-1} gradually decreased, while the band around 1500 cm^{-1} increased.

The broad conclusion from the difference spectra is that ordered β -turn and/or weak β -sheet structures develop with time from a predominantly disordered starting structure, and that the rate of increase in the order increases with increasing temperature (see below). This agrees with our observations on other proteins such as regenerated silk films.

Intensity-time plots generated from the difference spectra from 40 to 100 °C at 1700 cm^{-1} , 1650 cm^{-1} , 1550 cm^{-1} and 1500 cm^{-1} were used to study the conformation transition kinetics. Fig. 2 shows the effect of different temperatures on the normalized Δ absorbance-time curves at 1500 cm^{-1} (Fig. 2a) and 1550 cm^{-1} (Fig. 2b) of the soybean protein thin films to illustrate the kinetics of the conformational changes, which is typical of all the frequencies measured. Fig. 2a shows that there was a progressive slowing in conformational changes at lower temperatures. The kinetics of conformational changes showed a good fit with the first-order exponential growth function of Eq. (1):

$$y = 1 - \exp\left(-\frac{t}{\tau(T)}\right) \quad (1)$$

where y denotes the normalized Δ absorbance in the difference spectra, t denotes the experimental time, and $\tau(T)$ is a temperature dependent relaxation time parameter.

From the best-fit relaxation rate at each temperature and for all four of the main difference spectra peak frequencies, Fig. 3 plots the relationship between relaxation rate $1/\tau(T)$, and temperature. It suggests a simple linear temperature dependence of rate, where conformation changes are activated at temperatures above about 35 °C.

3.2. Low temperature TGA analysis

In order to investigate the hypothesis that the kinetics shown in the FTIR analysis might be due to loss of water, the rate of water loss from the samples was measured as a function of temperature using TGA, mainly at low temperatures. We have already shown that thermal degradation of the soybean protein starts at about 250 °C and has a maximum rate at about 300 °C, depending upon the rate of heating [33], but water loss is likely to occur below 100 °C, so the current measurements were focused mainly upon the range 20–100 °C.

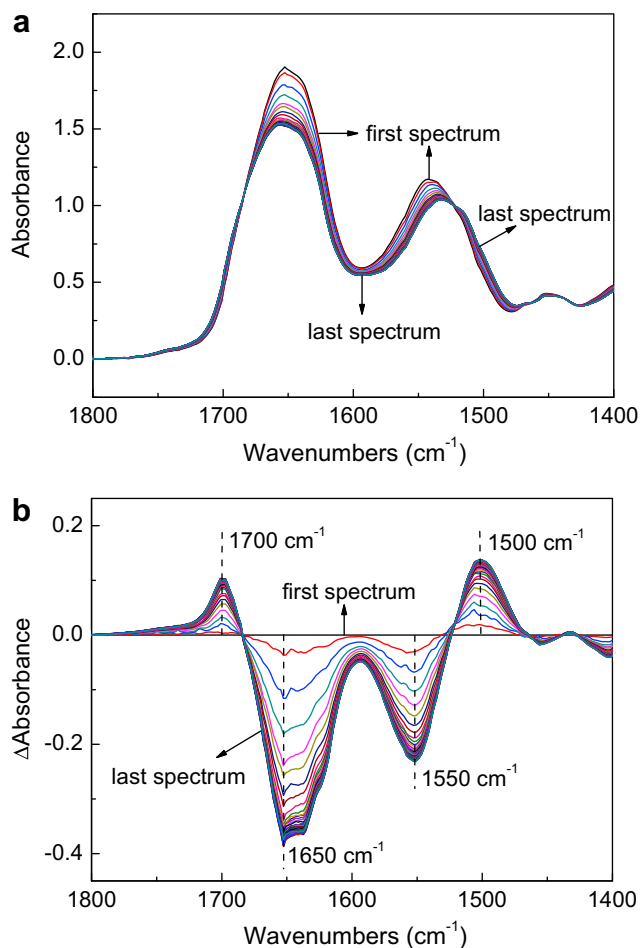


Fig. 1. Original FTIR spectra (a) and difference spectra (b) of soybean protein film with temperature maintained at 100 °C.

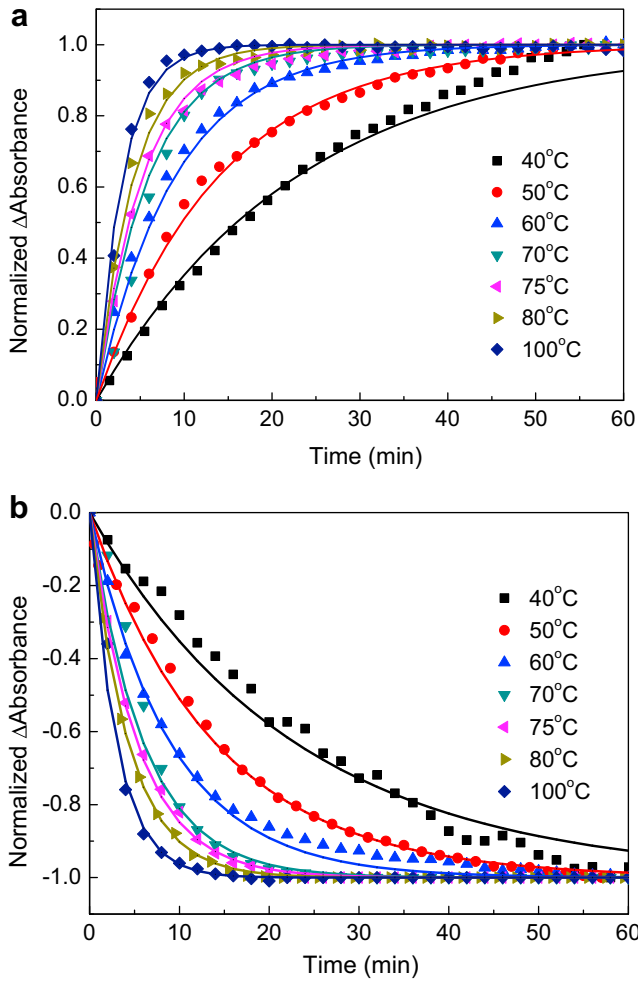


Fig. 2. Normalized Δ absorbance of soybean protein films at 1500 cm^{-1} (a) and 1550 cm^{-1} (b) as a function of time under isothermal conditions at temperatures as marked. Points are experimental measurements and lines are the same best-fit simple exponential relaxation model for all the four main difference spectra peaks.

The total water loss from the pre-dried soy films was in the range 5–6% by weight, with some of the water being lost in the drying phase at $20\text{ }^\circ\text{C}$ and the rapid heating phase to the isothermal temperature where data was recorded. Fig. 4 shows the fraction of

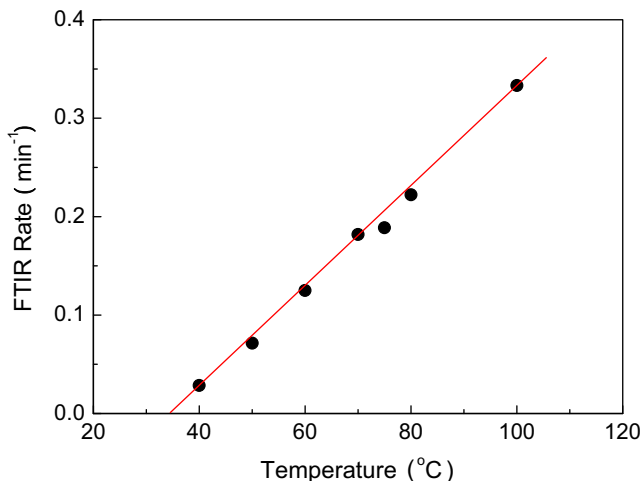


Fig. 3. Best linear fit of initial relaxation rate as a function of temperature from Fig. 2.

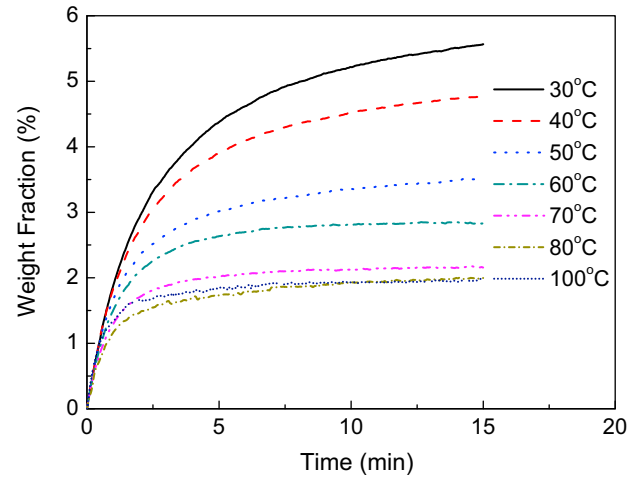


Fig. 4. Isothermal TGA plots of water loss from soybean protein films.

the water loss as a function of time over a range of isothermal conditions after drying, with the greater water loss during the pre-measurement equilibration process resulting in a lower apparent loss of water at higher temperatures.

Like the FTIR results, the isothermal TGA analyses show an exponential relaxation process that is faster at higher temperatures. If α is the water fraction from an initial fraction α_0 at any temperature T , and time t , the rate of loss is proportional to both α and a temperature dependent rate function $R(T)$ (Eq. (2)), assuming that the changes in structure with time do not significantly change the evaporation rate.

$$\frac{d\alpha}{dt} = \alpha \cdot R(T) \rightarrow \alpha = \alpha_0 \left[1 - \exp\left(-\int_0^t R(T) dt\right) \right] \quad (2)$$

Fig. 5 shows the initial rate of change in TGA water loss, $R(T)$, as a function of temperature under isothermal conditions, with all the curves normalized relative to the maximum water loss α_0 . The rate function $R(T)$ is best fitted from the experimental results as a simple linear relation in temperature, starting at the freezing point of water.

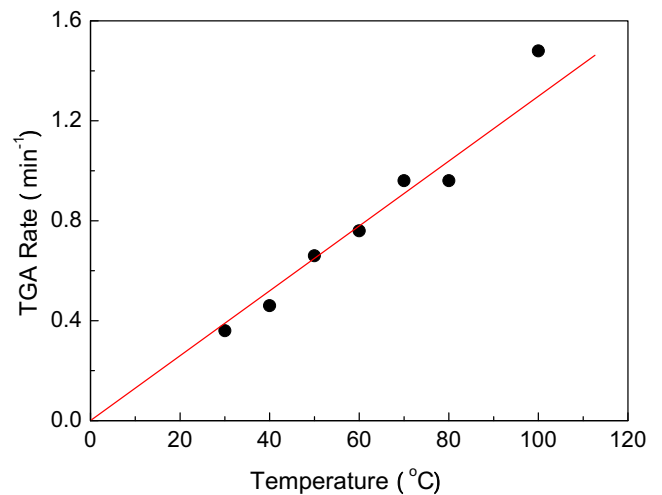


Fig. 5. Initial fractional rate of TGA water loss as a function of temperature in the soybean protein films under isothermal conditions. Points are taken from the normalized experimental data, and line is a best-fit linear model forced through zero.

To test the relatively simple linear temperature dependence of the water evaporation rate, Fig. 6 compares model predictions of evaporation rate with observation in four non-isothermal TGA experiments using Eq. (2), with $R(T) = 0.0134T$ taken directly from the linear fit in Fig. 5 and $\alpha_0 \approx 0.03$ from the maximum water fractions lost. The linear heating rates $r(t)$ of 2, 5, 10, and 20 °C/min have an expression for temperature T (°C), as a function of time t (Eq. (3)):

$$T = 20 + t \cdot r(t) \quad (3)$$

3.3. Dynamic mechanical thermal analysis

To further characterize the structural relaxation processes found in FTIR experiments, we looked at the relaxation characteristics of the soybean protein films using DMTA, as described under experimental methods. Since the dry films were so brittle, the samples were held in a powder tray clamp, in which multiple films are clamped between metal plates and subjected to constrained bending deformation. Under such conditions, the absolute values of loss tangent and storage modulus are not useful, but the position and distribution of the loss tangent peaks give important information about the relaxation processes in the polymer; for example, the main glass transition temperature, $T_g = 487$ K (214 °C), as shown in Fig. 7.

At temperatures well below T_g , the loss peaks were varied and depend very much on the effective drying conditions of the film during their processing and test history (very simply, drier films give smaller peaks in the range 0–100 °C), but the 214 °C peak was very reproducible and could be modelled as a normal distribution with a standard deviation of 10°, superimposed upon a baseline loss tangent of 0.011.

The key point about this DMTA information is that it gives an indication of dynamic relaxation processes, relative to which we can compare the relaxation events observed by FTIR. In Fig. 7, we have fitted two Gaussian loss peaks to the experimental data at higher water levels, which have peak positions at 7 and 75 °C and a standard deviation of 25°. We suggest that these peaks are associated with water molecules hydrogen bonded to the amide groups in the protein chain backbone [17]. The most important region is labelled 'water 1', which we suggest is one water molecule per amide group and which is the relaxation envelope in temperature where the water-amide interactions go through an elastic instability

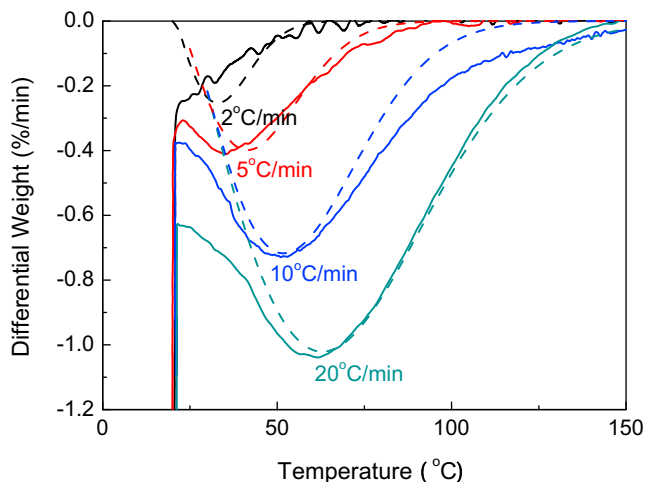


Fig. 6. Comparison of model (dashed lines) and observed (solid lines) rates of water loss under non-isothermal conditions at heating rates as marked in degrees per minute.

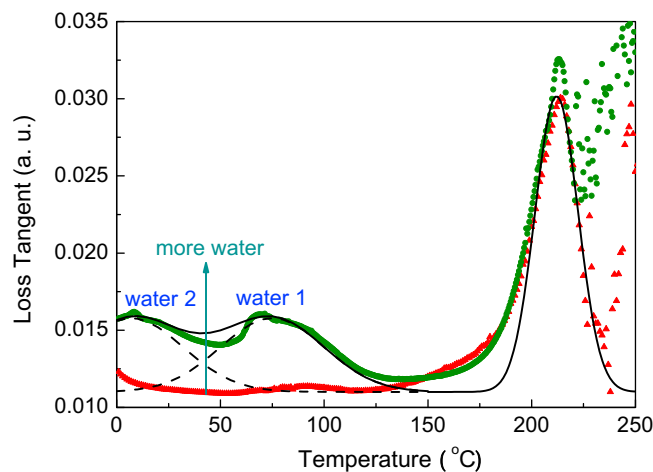


Fig. 7. DTMA scan of soy films: points are experimental measurements on desiccated (\blacktriangle) and lightly hydrated (\bullet) soybean protein films; solid line is a simplified model distribution; dashed lines are model distributions for suggested water contributions that are superimposed upon the underlying dry protein response, labelled water 1 and water 2.

condition, which means that the amide groups become mobile and can potentially reform interactions with neighbouring chains in new configurations [24]. Therefore, as temperature increases through the 'water 1' loss peak, more amide groups can reconfigure for a faster cooperative rate of conformation change, depending also upon the mobility and interactions with water molecules. We associate the 'water 2' peak with loosely bound water around the amide group. For reference, we have recently presented a more general discussion on the effect of water on the glass transition temperature in proteins such as natural silk [34].

4. Discussion

The results of FTIR, TGA, and DMTA analyses of the same soybean protein film samples all show kinetic processes occurring in the temperature range from 0 to 100 °C. However, the kinetics of water loss from TGA observations do not appear correspond directly with the kinetics of conformational changes suggested by FTIR and DMTA observations. Fig. 8 compares the TGA and FTIR normalized rates as approximately linear functions of temperature from Figs. 3 and 5, but with different starting temperatures at zero rate.

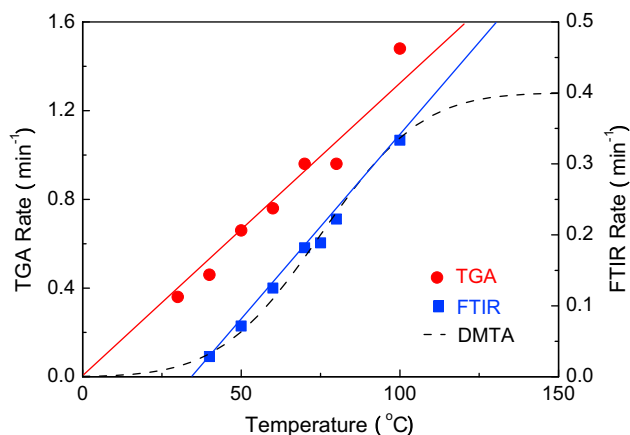


Fig. 8. Comparison of the normalized rates from TGA and FTIR experiments (taken from Figs. 3 and 5, with experimental points and best linear fits to the data) with a cumulative distribution of a model loss peak of 'water 1' from DMTA observations (dash line) in Fig. 7. The DMTA cumulative probability distribution is scaled by a factor 0.4 min^{-1} as a rate function to best-fit the FTIR rate data (see text).

Also in Fig. 8, a cumulative normal distribution function is plotted for the ‘water 1’ DMTA loss peak shown in Fig. 7, which is scaled by a factor 0.4 min^{-1} to best fit the FTIR rate data. This distribution function reflects the cumulative fraction of the molecular groups that have undergone a dynamic transition or relaxation process up to that temperature, which we have associated with a single water molecule that is hydrogen bonded to the main chain polar amide groups in the protein. This process is physically the same as the denaturing process that has been modelled quantitatively in previous work as an elastic instability of water–amide interactions, with the same fundamental mechanism as a glass transition temperature [24]. The onset of mobility in the water molecules allows the amide groups to reconfigure and form stronger amide–amide hydrogen bonds. Thus, simple loss of water (evaporation) is insufficient by itself to allow the protein chains to reconfigure, which requires an activation step for the water to become mobile.

From the above discussion, the link between the different relaxation processes and their absolute time scales is still quite vague. A connection is now needed between the kinetic observations presented here and the theory and observations on thermo-physical properties of proteins discussed in the introduction. To do this, the DMTA relaxation events on a scale of seconds associated with the fraction of local water–amide transition events must be transformed into cooperative conformational changes in the protein chains on a scale of minutes.

The bound ‘water 1’ loss peak in Fig. 7 was analyzed as a normal distribution with a mean position at 75°C and a standard deviation of 25° . If we take the cumulative distribution, this represents the cumulative fraction of the peptide segments that can release the ‘bound’ water as a function of temperature in any given time. This is plotted in Fig. 8 as a line that is scaled by a factor 0.4 min^{-1} to best fit the FTIR rate data. From this, we can estimate a characteristic relaxation time τ of about 150 s (2.5 min) for the bound water fraction to become mobile in our experiments, bearing in mind the variability in the samples and relaxation data. Does this relaxation time have any physical meaning? Here we use the approach of group interaction modeling, GIM, of Porter to relate the fraction of local transition events to the cooperative relaxation time of cooperative skeletal mode events for conformational changes using structural parameters (such as the Debye temperature for skeletal mode vibrations, θ_1) that can also be quantified independently through thermal analysis [35].

From the TGA measurements, a typical water fraction in the protein is 5% by weight. Using a generic model poly(alanine) structure for the protein with a segment molecular weight of 73 Da [22], the number fraction of the amide groups that have one hydrogen bonded water molecule is 0.2. If we take this as the cumulative fraction of the polymer that goes through a local transition process well below the main glass transition temperature of $486 \text{ K} = 213^\circ\text{C}$, we need to estimate the characteristic relaxation time of the polymer with this fraction of dynamic rubber-like states around T_g , to which we assign a value by convention of $\tau(T_g) = 1 \text{ s}$ [24].

Using the GIM normal distribution function for the glass transition zone with an intrinsic standard deviation of $s = 6^\circ$, the cumulative fraction of polymer that has become mobile due to the water transition events, $p(T_e) = 0.2$, is equivalent to a polymer with an effective temperature T_e that is 5° below T_g (Eq. (4)).

$$p(T_e) = 0.2 = \int_0^{T_e} \frac{1}{s\sqrt{2\pi}} \exp\left(-\frac{(T_e - T_g)^2}{2s^2}\right) dT \quad (4)$$

We can now estimate the relaxation time of cooperative glass

transition events associated with this fraction at an equivalent temperature $T_e = T_g - 5$ using a Doolittle-type function with the parameter value $\theta_1 = 400 \text{ K}$ (Eq. (5)).

$$\tau(T) \approx \tau_0 \exp\left(-\frac{1280 + 50 \ln \theta_1}{T_e - T_g + 50}\right) \approx 10^{-13} \exp\left(-\frac{1580}{T_e - T_g + 50}\right) (\text{s}) \quad (5)$$

where $\tau_0 \approx 10^{-13} \text{ s}$ is the characteristic time for skeletal mode vibrations and is given in terms of the Planck and Boltzmann constants h and k respectively by Eq. (6):

$$\tau_0 = \frac{h}{k\theta_1} \quad (6)$$

which gives $\tau(T_g - 5) = 150 \text{ s}$ as the expected shortest relaxation time of the hydrated soybean protein with about 5% water content in this work. Clearly, this relaxation time will reduce with increasing water content and increase as the active water fraction decreases. This relaxation time corresponds to a rate scaling factor ($1/\tau(T_g - 5)$) in the cumulative distribution model fit in Fig. 8 of 0.4 min^{-1} , which happens to agree with the scaling factor of 0.4 min^{-1} used to fit the model curve, although this scaling of time is meant only to be a first general suggestion. Thus, we see that the water content may be interpreted physically as giving a dynamic fraction of the protein polymer that can reconfigure cooperatively at the temperatures and in the time scales in our experiments.

Taken together, the FTIR and the DMTA observations combine to suggest that the onset of mobility of water associated with the protein amide groups controls the kinetics of configuration changes, whereas the TGA observations more simply reflect the kinetics of water evaporating from the samples, which may in some way be related back to the activation of mobility. We feel that understanding the difference in these kinetic processes is important for understanding the role of water in regulating the time-dependent evolution of conformations and secondary structures in proteins, which dictates their physical properties. For example, increasing the fraction of crystalline β -structures dramatically increases the rigidity of the material and reduces its sensitivity to water uptake.

5. Conclusions

By comparing the kinetics of protein–water interactions as a function of temperature using time-resolved FTIR, TGA, and DTMA measurements on soybean protein films, we have shown that simply evaporating water from the film (TGA) is insufficient to explain the rate of conformational changes (FTIR and DMTA). We suggest that an elastic instability condition of denaturation or glass transition events in water–amide interactions is the governing mechanism for conformational changes that allows the evolution of disordered structures into more ordered secondary structures, thereby controlling the changes in physical properties such as stiffness and water sensitivity.

Acknowledgements

XC would like to thank the National Natural Science Foundation of China (No. 20674011), the Program for New Century Excellent Talents in University of MOE of China (NCET-06-0354) and the Program for Changjiang Scholars and Innovative Research Team in University of MOE of China (IRT-06-12) for financial support. DP would like to thank support from the European Research Council (SP2-GA-2008-233409) and AFOSR (F49620-03-1-0111). Thanks to

Dr. Christopher Holland for DMTA analyses, and Dr. Yuhong Yang and Dr. Lei Huang for valuable discussions.

References

- [1] Thiering R, Hofland G, Foster N, Witkamp G, Wielen L. *Biotech Prog* 2001;17(3):513–21.
- [2] Chang CY, Duan B, Zhang LN. *Polymer* 2009;50(23):5467–73.
- [3] Feng ZC, Shao ZZ, Yao JR, Huang YF, Chen X. *Polymer* 2009;50(5):1257–63.
- [4] Shang J, Shao ZZ, Chen X. *Polymer* 2008;49(25):5520–5.
- [5] Kinsella JE. *J Am Oil Chem Soc* 1979;56(3):242–58.
- [6] Su JF, Huang Z, Yang CM, Yuan XY. *J Appl Polym Sci* 2008;110(6):3706–16.
- [7] Su JF, Wang XY, Huang Z, Yuan XY, Li M, Xia WL, et al. *J Appl Polym Sci* 2010;115(3):1901–11.
- [8] Park SK, Hettiarachchy NS, Were L. *J Agric Food Chem* 2000;48(7):3027–31.
- [9] Gao CL, Stading M, Wellner N, Parker ML, Noel TR, Mills ENC, et al. *J Agric Food Chem* 2006;54(13):4611–6.
- [10] Choi SG, Kim KM, Hanna MA, Weller CL, Kerr WL. *J Food Sci* 2003;68(8):2516–22.
- [11] Subirade M, Kelly I, Gueguen J, Pezolet M. *Int J Biol Macromol* 1998;23(4):241–9.
- [12] Chen X, Shao ZZ, Marinkovic NS, Miller LM, Zhou P, Chance MR. *Biophys Chem* 2001;89(1):25–34.
- [13] Chen X, Knight DP, Shao ZZ, Vollrath F. *Biochemistry* 2002;41(50):14944–50.
- [14] Chen X, Shao ZZ, Knight DP, Vollrath F. *Proteins* 2007;68(1):223–31.
- [15] Sun BJ, Li WZ, Wu PY. *Polymer* 2008;49(11):2704–8.
- [16] Hu X, Kaplan DL, Cebe P. *Macromolecules* 2006;39(18):6161–70.
- [17] Pyda M, Hu X, Cebe P. *Macromolecules* 2008;41(13):4786–93.
- [18] Hu X, Kaplan DL, Cebe P. *Macromolecules* 2008;41(11):3939–48.
- [19] Wunderlich B, Cheng SZD, Loufakis K. *Thermodynamic properties in encyclopedia of polymer science and engineering*, vol. 16. New York: Wiley Interscience; 1989.
- [20] Porter D. *Group interaction modelling of polymer properties*. New York: Marcel Dekker; 1995.
- [21] Porter D, Gould PJ. *Int J Solid Struct* 2009;46(9):1981–93.
- [22] Vollrath F, Porter D. *Appl Phys A* 2006;82(2):205–12.
- [23] Vollrath F, Porter D. *Soft Matter* 2006;2(5):377–85.
- [24] Porter D, Vollrath F. *Soft Matter* 2008;4(2):328–36.
- [25] Guan J, Tian K, Yao JR, Shao ZZ, Chen X. *Acta Polym Sinica* 2010;2:250–4.
- [26] Chen X, Knight DP, Shao ZZ. *Soft Matter* 2009;5(14):2777–81.
- [27] Goormaghtigh E, Cabiaux V, Ruyschaert JM. *Eur J Biochem* 1990;193(2):409–20.
- [28] Barth A, Zscherp C. *Q Rev Biophys* 2002;35(4):369–430.
- [29] Barth A. *Biochim Biophys Acta-Bioenerg* 2007;1767(9):1073–101.
- [30] Zhou W, Chen X, Shao ZZ. *Prog Chem* 2006;18(11):1514–22.
- [31] Riblett AL, Herald TJ, Schmidt KA, Tilley KA. *J Agric Food Chem* 2001;49(10):4983–9.
- [32] McGrath K, Kaplan DL. *Protein-based materials*. Boston: Birkhauser Press; 1996. 103–133.
- [33] Porter D, Vollrath F, Tian K, Chen X, Shao ZZ. *Polymer* 2009;50(7):1814–8.
- [34] Fu CJ, Porter D, Shao ZZ. *Macromolecules* 2009;42(20):7877–80.
- [35] Reference [20]: section 2.5.4 for low temperature relaxations; sections 3.4.3 and 3.4.6 for relaxation time and distribution.